

# An IR, NMR, dipole moment and X-ray study on intramolecular O–H...N hydrogen bonding in 8-hydroxy-*N,N*-dimethyl-1-naphthylamine

E. Grech,<sup>a</sup> J. Nowicka-Scheibe,<sup>a</sup> Z. Olejnik,<sup>b</sup> T. Lis,<sup>b</sup> Z. Pawelka,<sup>b</sup> Z. Malarski<sup>b</sup> and L. Sobczyk<sup>\*,b</sup>

<sup>a</sup> Institute of Fundamental Chemistry, Technical University, 71-065 Szczecin, Poland

<sup>b</sup> Institute of Chemistry, University of Wrocław, F. Joliot-Curie 14, 50-383 Wrocław, Poland

The X-ray diffraction structure at 85 K and physico-chemical properties of 8-hydroxy-*N,N*-dimethyl-1-naphthylamine have been studied. Five crystallographically independent molecules, of which two are disordered, are contained in the centrosymmetric triclinic unit cell of dimensions:  $a = 10.307(9)$ ,  $b = 13.459(9)$ ,  $c = 19.183(9)$  Å,  $\alpha = 93.98(6)$ ,  $\beta = 102.91(6)$ ,  $\gamma = 97.05(9)^\circ$ ,  $V = 2561(3)$  Å<sup>3</sup>. For the non-disordered molecules the mean length of the intramolecular O–H...N hydrogen bond is 2.569(5) Å and the H atom position is described by the 0.90(3) and 1.72(3) Å mean distance for O–H and H...N, respectively. Two of the crystallographically independent molecules are joined by a weak, bifurcated O–H...O hydrogen bond with O...O distance of 2.878(2) Å. The studies of <sup>1</sup>H NMR, IR spectra and dipole moments indicate the presence of fairly strong O–H...N hydrogen bonding. The dipole moments and <sup>1</sup>H NMR data in cyclohexane, CCl<sub>4</sub>, benzene and dioxane show weak association, particularly in cyclohexane and CCl<sub>4</sub>. The results demonstrate that association leads to the formation of non-polar dimers. In dioxane a complexation with the solvent molecules takes place without the breaking of intramolecular hydrogen bonds.

8-Hydroxy-*N,N*-dimethyl-1-naphthylamine (HDN) belongs to the interesting group of compounds containing intramolecular O–H...N hydrogen bonding. The presence of such bonding is reflected in a number of properties. There is a remarkable lowering of the proton transfer rate constant to  $3 \times 10^6$  m<sup>3</sup> kmol<sup>-1</sup> s<sup>-1</sup> which is four orders of magnitude lower than that governed by diffusion (*ca.*  $10^{10}$  m<sup>3</sup> kmol<sup>-1</sup> s<sup>-1</sup>).<sup>1</sup> The equilibrium constant for the breaking of the O–H...N bridge can be estimated to be  $3 \times 10^{-4}$  and is greater by only one order of magnitude than that for the strong intramolecular NHN<sup>+</sup> hydrogen bridge formed in the protonated proton sponge 1,8-bis(dimethylamino)naphthalene.<sup>1</sup> The strength of the hydrogen bonding in HDN is also reflected in the enhancement of the p*K*<sub>a</sub> value which appeared to be six orders of magnitude higher than that for 1-naphthol.<sup>1</sup>

The O–H...N hydrogen bonding in HDN can be classified as medium-strong as shown by the range of  $\nu_{\text{OH}}$  stretching vibrations in the IR spectra and the position of the bridge proton <sup>1</sup>H NMR signal at  $\delta$  13.6.<sup>1</sup>

These data prompted us to undertake more detailed studies of the O–H...N bridge in HDN, in particular the environment and concentration effects on the IR and <sup>1</sup>H NMR spectra as well as the dipole moment. Particularly important, it seemed to us, would be the X-ray diffraction studies to obtain information about the structure of HDN and the geometry of the O–H...N hydrogen bonds.

## Experimental

Electric permittivities were measured by the superheterodyne beat method using a WTW DM01 DIPOLMETER. The electric capacity was measured with an accuracy of  $\Delta C/C \leq 1 \times 10^{-4}$ . The solution density was determined pycnometrically with an accuracy of  $\pm 1 \times 10^{-1}$  kg m<sup>-3</sup> and the refractive index for the D-line of sodium was measured using an Abbe refractometer to an accuracy of  $\pm 5 \times 10^{-5}$ . All the measurements were performed at 298 K.

The molar dipole polarization of the solute was calculated in

terms of the Onsager local field model using eqn. (1)<sup>2</sup> where the

$$P = \frac{(\epsilon_1 - n_1^2)(2\epsilon_1 + n_1^2)M_1}{\epsilon_1(n_1^2 + 2)^2d_1} \times \left( \frac{\alpha\epsilon_1 - \gamma n_1^2}{\epsilon_1 - n_1^2} + \frac{2\alpha\epsilon_1 + \gamma n_1^2}{2\epsilon_1 + n_1^2} - \frac{2\gamma n_1^2}{n_1^2 + 2} - \alpha - \beta + \frac{M_2}{M_1} \right) \quad (1)$$

subscripts 1 and 2 refer to the solvent and solute, respectively. The coefficients  $\alpha$ ,  $\beta$  and  $\gamma$  were calculated using the Hedstrand procedure.<sup>3</sup>

<sup>1</sup>H NMR spectra were recorded on a TESLA BS567A (100 MHz) spectrometer at 303 K. For the determination of the chemical shifts in CCl<sub>4</sub>, TMS was used as an internal standard. For other solvents their <sup>1</sup>H signals were used as a reference.

IR spectra of solid HDN in KBr pellets were recorded over the range 400–4000 cm<sup>-1</sup> with a Perkin-Elmer 180 spectrophotometer. IR spectra of solutions in CCl<sub>4</sub> were recorded in the range 1600–4000 cm<sup>-1</sup> for 1.0 and 0.04 kmol m<sup>-3</sup> concentrations with CsI cells of 0.12 and 3.01 mm thickness, respectively (with compensation for solvent absorption).

## Materials

HDN was synthesized according to ref. 4. The solvents used (cyclohexane, CCl<sub>4</sub>, benzene and dioxane) were purified by using standard methods<sup>5</sup> and dried over sodium or 4 Å molecular sieves.

## Crystallography

The compound was crystallized from CCl<sub>4</sub>, C<sub>2</sub>H<sub>5</sub>OH, CH<sub>3</sub>OH, ethyl acetate, toluene, benzene, propan-1-ol and other solutions. In all cases the same crystalline form was obtained.

Measurements were performed with the Syntex P2<sub>1</sub> diffractometer (room temperature) and with the Kuma  $\kappa$ -geometry diffractometer equipped with a liquid-nitrogen-cooling device (low temperature). Graphite-monochromatized

**Table 1** Crystal data for 8-hydroxy-*N,N*-dimethyl-1-naphthylamine

General formula	C <sub>12</sub> H <sub>13</sub> NO
<i>M<sub>r</sub></i>	187.24
Space group	<i>P</i> $\bar{1}$
<i>a</i> /Å	10.307(9) [10.448(6)] <sup>a</sup>
<i>b</i> /Å	13.459(9) [13.592(7)]
<i>c</i> /Å	19.183(9) [19.480(9)]
$\alpha$ /°	93.98(6) [94.60(4)]
$\beta$ /°	102.91(6) [102.69(4)]
$\gamma$ /°	97.05(9) [97.83(4)]
<i>V</i> /Å <sup>3</sup>	2 561(3) [2 656(3)]
<i>T</i> /K	85(2) [298(1)]
<i>Z</i>	10
<i>D<sub>x</sub></i> /Mg m <sup>-3</sup>	1.214 [1.170]
<i>D<sub>m</sub></i> /Mg m <sup>-3</sup>	[1.175]
<i>F</i> (000)	1000
$\mu$ /mm <sup>-1</sup>	0.077 [0.075]
$\lambda$ , Å	0.710 69
Size/mm	0.8 × 0.4 × 0.3

<sup>a</sup> Crystal data at room temperature are given in square brackets.

Mo-K $\alpha$  radiation was used. The lattice parameters were determined from 48 reflections ( $10 < \theta < 13$ ) and from 15 reflections ( $10 < \theta < 18$ ), for 85(2) and 298(2) K, respectively. Crystal data are summarized in Table 1.

The structure was initially measured at 298 K and the SHELXL 86 program<sup>6</sup> was used for structure determination. The temperature factors for two of the five independent molecules showed large values suggesting a disorder which could not be resolved. Therefore, a second data set of 10 452 reflections was collected at 85 K. The 5796 unique reflections with  $I > 3\sigma(I)$  were used in the calculations. Starting refinement with the room-temperature parameters, the relatively high peaks near atoms of one molecule remained present in the difference map. At first, a model with six molecules was used. In this model two molecules with a population of *ca.* 50%, sharing approximately the same site, were refined independently. Next, because the difference map revealed a slight disorder of another molecule, the model with seven molecules was assumed. In this model one of the two sites showing disorder is occupied by the molecules 4 and 5 and another site is occupied by the molecules 6 and 7 (see Fig. 6 below). The site occupation factors, refined together for molecules 4 and 7 and for molecules 5 and 6 were 47 and 53%, respectively. In the refinement, chemically equivalent bonds of all disordered molecules were restrained to be approximately equal by using a standard procedure of the SHELXL 93 program<sup>7</sup>. All non-hydrogen atoms were refined anisotropically. The hydrogen atoms were included using a riding model (a rotation for the hydroxy and methyl groups was allowed) with the individual temperature factors 1.2 times  $U_{eq}$  of the parent atoms. Positions of the hydroxy hydrogen atoms for non-disordered molecules were next refined. Full-matrix least-squares refinement on  $F^2$  of 911 parameters converged at  $R = 0.0464$  and  $R_w = 0.1227$  with a calculated  $w = 1/[\sigma^2(F^2) + (0.0736P) + 1.19P^2]$  where  $P = (F_o^2 + 2F_c^2)/3$ . The final electron density was between  $-0.19$  and  $0.37$  e Å<sup>-3</sup>.

The model with six molecules was fortunately used to refine the structure measured at 298 K [ $R = 0.0529$  for 3888 reflections with  $I > 3\sigma(I)$ ]. Non-essential differences in the geometries of the non-disordered molecules were found between the structure at 298 and 85 K. A thermal shortening (by 1–3  $\sigma$ ) of all bond lengths and a lengthening of the intermolecular O...O distance in the hydrogen bonding between molecules 2 and 3 are observed at 298 K. Scattering factors were taken from *International Tables for X-Ray Crystallography*.<sup>8</sup>

Atomic coordinates, bond lengths and angles and thermal

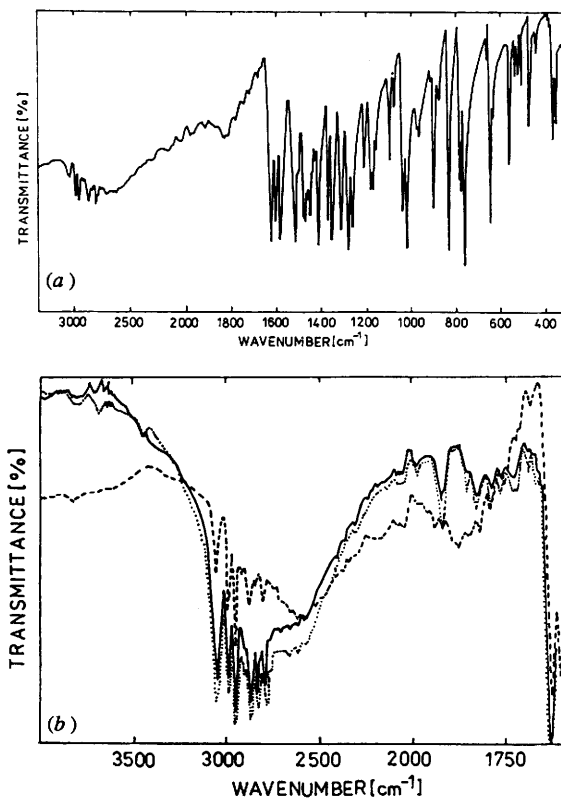


**Fig. 1** IR spectrum of 8-hydroxy-*N,N*-dimethyl-1-naphthylamine in (a) KBr pellet and (b) comparison of spectra in the  $\nu_{OH}$  region for the solid state (---), CCl<sub>4</sub> solution  $c = 1$  mol dm<sup>-3</sup> (—) and  $c = 0.04$  mol dm<sup>-3</sup> (···)

parameters have been deposited with the Cambridge Crystallographic Data Centre.†

## Results and discussion

### IR spectra

The characteristic features of the IR spectra of HDN are as follows. The  $\nu_{OH}$  stretching vibration band is very intense and broad and its maximum is located at  $2760$  cm<sup>-1</sup> in CCl<sub>4</sub>. On dilution, in the concentration range  $0.04$ – $1$  mol dm<sup>-3</sup> in CCl<sub>4</sub>, this band remains unchanged. These facts show that we are dealing with a medium–strong hydrogen bond without  $\pi$ -electron conjugation contributing to this bond. It is known that the presence of such conjugation leads to a substantial reduction in the absorption intensity. This band can be compared with those formed by phenols of low acidity with amines and also with those formed in *ortho* Mannich bases.<sup>9</sup>

In Fig. 1 are shown the spectra of HDN in CCl<sub>4</sub> and in the solid state (KBr discs). In the finger-print region we do not find remarkable differences. However, a marked influence of the environment is observed in the region of  $\nu_{OH}$  vibrations when comparing the solution to the solid state; in the latter, remarkable broadening of this band and the appearance of a broad doublet takes place. The main maximum is located at  $2600$  cm<sup>-1</sup> and the second one at  $1870$  cm<sup>-1</sup> with some fine structure. One notices that weak peaks are observed already in the solution spectra (overtones and summation frequencies). The reason for the doublet of the  $\nu_{OH}$  band in solid HDN is not clear. The most probable source of the creation of a doublet is a Fermi resonance with  $2\delta_{OH}$  which corresponds to the minimum at *ca.*  $2000$  cm<sup>-1</sup>.

† Crystallographic data has been deposited. For details of the CCDC deposition scheme, see 'Instructions for Authors (1996)', *J. Chem. Soc., Perkin Trans. 2*, 1996, Issue 1.

There is no characteristic  $\delta_{\text{OH}}$  band of the hydrogen bonded OH group because of coupling with the  $\nu_{\text{CO}}$  mode. However we find absorption bands in the region close to  $1000\text{ cm}^{-1}$  which can be interpreted as being due to  $\delta_{\text{OH}}$  vibrations. The  $\gamma_{\text{OH}}$  vibration band is located at  $770\text{ cm}^{-1}$ . The studies at low temperatures of both  $\nu_{\text{OH}}$  and  $\gamma_{\text{OH}}$  bands in the range of 80–300 K allowed us to determine the average temperature coefficients  $\Delta\nu/\Delta T$  and  $\Delta\gamma/\Delta T$  to be  $0.35\text{ cm}^{-1}\text{ K}^{-1}$  and  $-0.05\text{ cm}^{-1}\text{ K}^{-1}$ , respectively. The bands related to  $\delta_{\text{OH}}$  vibrations are also sensitive to temperature with negative coefficients

### $^1\text{H}$ NMR spectra

The dependence of the location of the  $^1\text{H}$  magnetic resonance frequency on the concentration of HDN in cyclohexane,  $\text{CCl}_4$ , benzene and dioxane was measured. The resonance signals in all solvents show down-field shifts on dilution, but the dilution coefficient ( $\Delta\nu/\Delta c$ ) differs markedly depending on solvent. The strongest dependence of  $\delta$  on concentration is observed in cyclohexane and much weaker in benzene and dioxane. The dependence of frequency,  $\nu$ , on concentration and the calculated dilution coefficients are presented in Table 2. Also collected in Table 2 are the values of chemical shifts,  $\delta$  (in relation to TMS) extrapolated to infinite dilutions. The results clearly show the association of HDN, which, according to expectation, is most intensively reflected in the non-polar solvent, cyclohexane.

The chemical shift in HDN indicates that we are dealing with a fairly strong intramolecular  $\text{OH}\cdots\text{N}$  hydrogen bond, compared with that in *ortho* Mannich bases.<sup>10</sup> In those compounds we notice chemical shifts of the order of 13–14 ppm in  $\text{CCl}_4$ . Similar values should be seen in the complexes of phenols with amines when the proton is localized at the oxygen atom.<sup>11</sup>

### The dipole moment

The molar dielectric polarization of HDN was measured in the same solvents as for  $^1\text{H}$  NMR. The final results are presented in Table 3. In cyclohexane and  $\text{CCl}_4$  one observes the dependence of polarization on concentration. It is seen particularly clearly on the plot of  $\mu^2$  versus mole fraction,  $x$ , in Fig. 2. The dependence was approximated by means of a second-order polynomial and hence the values of  $P$  and  $\mu$  were evaluated for infinite dilution. In this way one obtains similar values of  $\mu$ , in the limits of experimental error, for the first three solvents. A slightly larger dipole moment ( $0.5 \times 10^{-30}\text{ C m}$ ) was obtained for HDN in dioxane.

The task was undertaken to evaluate the so-called polarity of the hydrogen bond, *i.e.* the interaction dipole moment assuming that this vector is located along the axis connecting the oxygen

**Table 2** Dilution coefficients ( $\Delta\nu/\Delta c$ ) and chemical shift,  $\delta_\infty$

Solvent	Concentration/ $10^{-2}\text{ kmol m}^{-3}$	$(\Delta\nu/\Delta c)/$ $\text{Hz m}^3\text{ kmol}^{-1}$	$\delta_\infty$
Cyclohexane	3.23–74.19	$-32.50^a$	12.86
$\text{CCl}_4$	5.66–69.70	$-17.74$	12.97
$[\text{}^2\text{H}_6]\text{Benzene}$	4.33–64.52	$-5.81$	14.33
Dioxane	14.47–98.11	$-4.90$	14.09

<sup>a</sup> By assuming the linear relationship between  $\delta$  and  $c$ .

**Table 3** Dipole moments of 8-hydroxy-*N,N*-dimethyl-1-naphthylamine in various solvents

Solvent	Concentration range, $x_2/10^3$	$\alpha\varepsilon_1$	$\beta$	$\gamma m_1^2$	$P/10^{-6}\text{ m}^3$	$\mu/10^{-30}\text{ C m}$
Cyclohexane	1.569–9.22		0.6441	0.8793	169.2	$9.53^a$
$\text{CCl}_4$	2.03–13.07		$-0.4889$	0.9840	182.4	$9.90^a$
Benzene	1.65–7.23	12.566	0.5381	0.8087	173.9	9.67
Dioxane	1.65–10.57	13.890	0.1501	1.1430	196.0	10.27

<sup>a</sup> Values extrapolated to infinite dilution.

and nitrogen atoms. To do this we need to know the dipole moments of 1-naphthol and *N,N*-dimethyl-1-naphthylamine themselves. The dipole moments of those compounds were calculated according to eqn. (1) on the basis of literature data corresponding to the concentration dependence of relative permittivity, density and refractive index.<sup>12,13</sup> These data are collected in Table 4.

The resultant moment of HDN was calculated by assuming that the moment of naphthol is directed to the C–O axis forming an angle of  $90^\circ$ , while the moment of *N,N*-dimethyl-1-naphthylamine is at an angle of  $139^\circ$  to the C–N axis. Thus the resultant calculated dipole moment of the HDN molecule is  $7.67 \times 10^{-30}\text{ C m}$ . The comparison of this value with the experimental dipole moment of HDN indicates that the enhancement of the dipole moment due to the hydrogen bond formation is  $2 \times 10^{-30}\text{ C m}$ . This is a typical value for a hydrogen bond of medium strength where the electrostatic effects predominate.<sup>14</sup>

An explanation is needed for the concentration dependence of polarization and  $^1\text{H}$  resonance frequency. These effects can be explained in terms of self-association of HDN which occurs particularly in non-polar solvents. The decrease in the effective dipole on increasing the concentration indicates that non-polar or weakly polar aggregates (most probably dimers) are formed. On the other hand the invariability of IR spectra in the region of the  $\nu_{\text{OH}}$  stretching vibration band indicates that the dilution does not lead to the breaking of hydrogen bonds. Thus the observed dependence of  $\mu^2$  on concentration can be explained simply as being due to the formation of non-polar cyclic dimers stabilized by the additional bifurcated intermolecular bonds according to structure I. As follows from the X-ray diffraction studies (see the next section) such dimers are formed in the crystalline lattice.

The association constant  $K_{\text{as}} = c_d/c_m^2$  can be estimated from the dipole moment measurements by assuming that dimers,

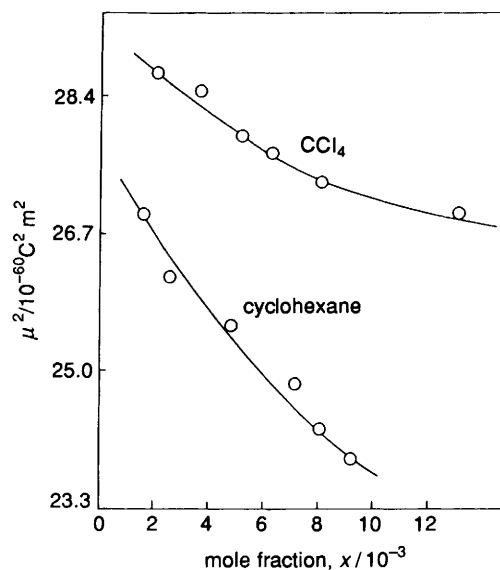
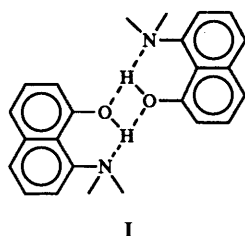


**Fig. 2** Plots of effective squares of the dipole moment  $\mu^2$  vs. concentration

**Table 4** Dipole moments of 1-naphthol and *N,N*-dimethyl-1-naphthylamine in benzene

Compound	Concentration range, $x_2/10^{-3}$	$\alpha\epsilon_1$	$\beta$	$\gamma n_1^2$	$P/10^{-6} \text{ m}^3$	$\mu/10^{-30} \text{ C m}$
1-Naphthol	3.32–17.18	3.670	0.4930	0.6143	45.6	4.93
<i>N,N</i> -Dimethyl-1-naphthylamine	6.19–34.52	2.131	0.3523	0.6673	22.3	3.47

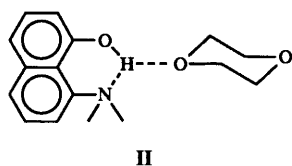


as centrosymmetric structures, are non-polar. The dipole polarization is then given by eqn. (2) where  $c$  is the total molar

$$P = P_m c_m / c \quad (2)$$

concentration of the compound ( $c = c_m + 2c_d$ ) and  $c_m$  and  $c_d$  are the concentration of monomer and dimer. The best agreement of the experimental dipole polarization as a function of concentration is obtained for  $K_{as} = 1.0$  and  $0.35 \text{ m}^3 \text{ kmol}^{-1}$  in cyclohexane and  $\text{CCl}_4$ , respectively. Extrapolated values of the dipole polarization to  $c_m/c = 1$  are essentially the same, *i.e.*  $170.8 \times 10^{-6}$  and  $179.7 \times 10^{-6} \text{ m}^3$  in cyclohexane and  $\text{CCl}_4$ , respectively. They are in a good agreement with those obtained from the extrapolation to infinite dilution.

There remains for explanation the comparison of the effects of dioxane and other solvents upon the dipole moment and chemical shift. The dioxane effect is accompanied by the increase (compared with that for cyclohexane and benzene) in dipole moments of  $0.7 \times 10^{-30} \text{ C m}$  and the chemical shift of 1.1 ppm. This is not due to the breaking of the  $\text{O-H} \cdots \text{N}$  intramolecular hydrogen bond, but due to a specific solvation with formation of a bifurcated hydrogen bond, structure II.



One should emphasize that the dioxane effect on the dipole moment of various compounds with intramolecular hydrogen bonds in most cases is of the order of *ca.*  $0.7 \times 10^{-30} \text{ C m}$ .

Special treatment is needed when the remarkable down-field shift of the bridge proton of HDN in benzene is considered. This effect should be ascribed to the aromatic solvent-induced shifts (ASIS) effect which cannot be parallel, as in our case, with the change of the dipole.

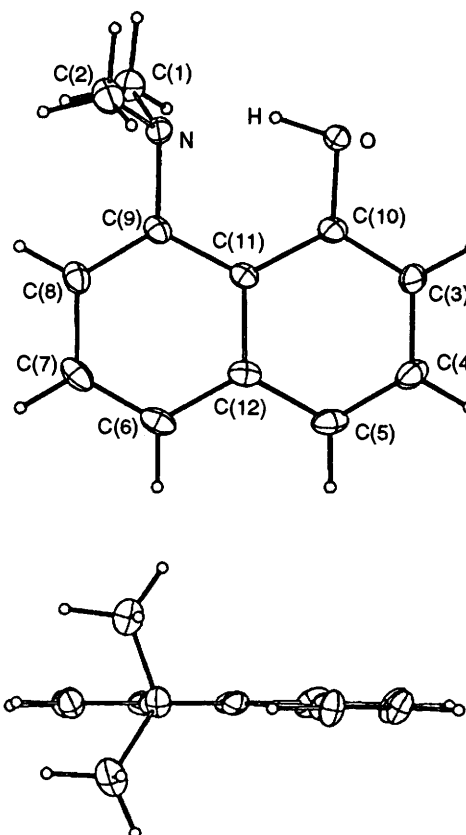
### X-Ray analysis

Formally, the crystal of HDN contains five crystallographically independent molecules in the asymmetric unit. However, to resolve a disordering observed in the structure it was necessary to assume the model with seven independent molecules. The molecules 1–3 are not disordered and the molecules 4–7, each of population near 50%, occupy two neighbouring sites in the crystal lattice. The bond distances and angles for 1–3 are equal within experimental error, thus in Table 5 only their mean values are presented. The bonding parameters for 4–7 are omitted because of a lower accuracy and will not be discussed in detail. ORTEP views of one representative molecule and the labelling scheme used for all molecules are presented in Fig. 3. In Fig. 4, where all independent molecules are superimposed by

**Table 5** Bond lengths (Å) and angles ( $^\circ$ ) averaged for three crystallographically independent molecules of 1-hydroxy-*N,N*-dimethyl-1-naphthylamine<sup>a</sup>

Bonds			
O–C(10)	1.353(8)	C(6)–C(12)	1.421(3)
N–C(9)	1.455(5)	C(6)–C(7)	1.363(3)
N–C(1,2)	1.467(4)	C(7)–C(8)	1.405(8)
C(3)–C(10)	1.370(5)	C(8)–C(9)	1.371(4)
C(3)–C(4)	1.400(1)	C(9)–C(11)	1.421(1)
C(4)–C(5)	1.366(1)	C(10)–C(11)	1.440(2)
C(5)–C(12)	1.412(3)	C(11)–C(12)	1.427(4)
Angles			
C(9)–N–C(1,2)	112.3(5)	C(8)–C(9)–N	121.4(2)
C(2)–N–C(1)	111.0(8)	C(11)–C(10)–C(3)	120.1(2)
C(10)–C(3)–C(4)	120.8(2)	C(11)–C(10)–O	120.8(5)
C(5)–C(4)–C(3)	121.0(2)	C(3)–C(10)–O	119.1(2)
C(12)–C(5)–C(4)	120.1(2)	C(12)–C(11)–C(9)	118.7(1)
C(12)–C(6)–C(7)	121.3(2)	C(12)–C(11)–C(10)	117.9(3)
C(8)–C(7)–C(6)	120.2(1)	C(9)–C(11)–C(10)	123.3(3)
C(9)–C(8)–C(7)	120.6(2)	C(11)–C(12)–C(5)	119.9(2)
C(11)–C(9)–C(8)	120.7(2)	C(11)–C(12)–C(6)	118.5(3)
C(11)–C(9)–N	117.9(2)	C(6)–C(12)–C(5)	121.6(4)

<sup>a</sup> The standard deviations of the averages given in parentheses are estimated as  $[\sum(x_i - \bar{x})^2/(n - 1)]^{1/2}$ . The individual esds for bonds are 0.004 Å and for angles 0.2 $^\circ$ .

**Fig. 3** ORTEP views of one representative molecule of 8-hydroxy-*N,N*-dimethyl-1-naphthylamine and the labelling scheme used for all crystallographically independent molecules (1–7)

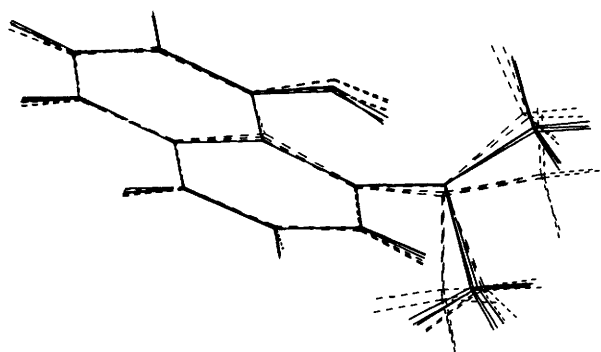


Fig. 4 Superposition of the crystallographically independent molecules of 8-hydroxy-*N,N*-dimethyl-1-naphthylamine. Dashed lines correspond to the disordered molecules.

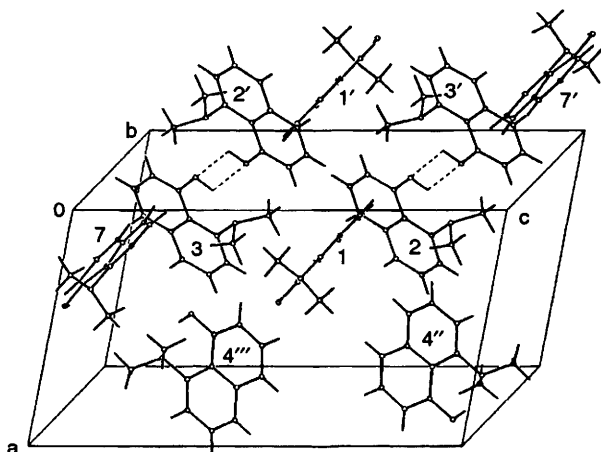


Fig. 5 Crystal packing. Only one molecule from each disordered pair is shown. Dashed lines correspond to the intermolecular hydrogen bonds. Symmetry code for molecules:  $'1 - x, -y, 1 - z$ ;  $''1 - x, 1 - y, 1 - z$ ;  $'''1 + x, 1 + y, z$ .

a fitting of the naphthalene carbons, the differences between their molecular conformations are visualized. As can be seen, the variations are associated with the position of the dimethylamino group in relation to the naphthalene core and are more marked for the disordered molecules. For the 1–3 molecules the torsional angles around  $C_{ring}-N$  deviate by  $10^\circ$  from  $60$  or  $120^\circ$ , whereas those around C–C do not differ from  $0$  or  $180^\circ$  by more than  $3.0(3)^\circ$ . Excluding the methyl groups, the molecules are only roughly planar [within  $0.043(3) \text{ \AA}$ , Fig. 3, for 1–3] exhibiting small but different deformations of naphthalene cores and different deviations of the nitrogen and oxygen atoms from the individual six-membered rings to which they are attached. The C–O distances equal  $1.361(3)$ ,  $1.343(3)$  and  $1.354(3) \text{ \AA}$  for 1, 2 and 3, respectively, are close to values of  $1.36 \text{ \AA}$  found for phenol.<sup>15</sup> On the other hand, the N– $C_{ring}$  distances are the same as those observed for the  $N(CH_3)_2$  substituent in a series of protonated  $DMANH^+$  cations with a strongly asymmetric hydrogen bridging.<sup>16–22</sup> Also, the mean N...O distance of  $2.569(5) \text{ \AA}$  is comparable to the N...N distance which varies from  $2.553$ – $2.654 \text{ \AA}$  in the  $DMANH^+$  series. The H atoms are bound to the oxygen atoms and their positions in relation to the dimethylamino group are almost the same for the molecules 1–3. The mean values of the O–H distances and H–O–C(10) angles are  $0.90(3) \text{ \AA}$  and  $106(1)^\circ$ , respectively; the N...H distances change from  $1.69(3)$  to  $1.75(3) \text{ \AA}$  and the O–H...N angles are in the range  $155(3)$ – $156(3)^\circ$ . The H...N–C angles are equal to  $96(1)^\circ$  for  $C_{ring}$  and range between  $109(1)$  and  $115(1)^\circ$  for  $C_{methyl}$ . The geometry of the naphthalene core is essentially similar to that observed in other 1,8-disubstituted naphthalenes. We note a small lengthening [by  $0.019(2) \text{ \AA}$ ] of the C(10)–C(11) bond with respect to the

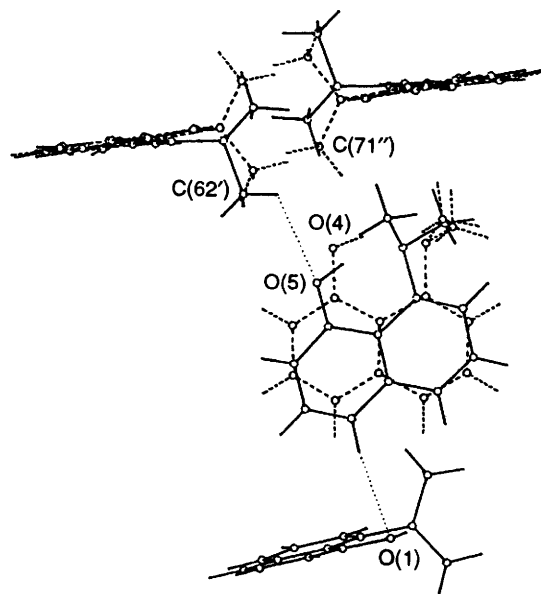


Fig. 6 Model of disordering. Dashed lines correspond to the molecules 4 and 7 with a population of 43%. Molecules 5 and 6 have a population of 53%. Intermolecular C–H...O interactions are indicated by dotted lines.

C(9)–C(11) bond, which can be a consequence of a greater electronegativity of OH compared with  $N(CH_3)_2$ . Furthermore, the angle C(9)–C(11)–C(10) of  $123.3(3)^\circ$  is significantly smaller than the mean value of  $125^\circ$  observed for  $DMANH^+$  derivatives. For 1,8-disubstituted naphthalenes a distortion of this angle from  $120^\circ$  is usually interpreted as the measure of the strain resulting from interactions between substituents and between substituents and the naphthalene core. Fig. 5 shows a packing diagram in which only one molecule from each disordered pair, namely 4 and 7, is present.

A pseudo-inversion centre about  $0, 1/2, 1/4$  exists relating 2 ( $-x, 1 - y, 1 - z$ ) to 3 and the averaged positions of 7 and 6 with 1 ( $-x, 1 - y, 1 - z$ ). Of course, such pseudo-inversion centres are also localized at the  $0, 1/2, 3/4$  site and other sites related by an inversion. The fifth molecule, 4 or 5 from a disordered pair, is displaced so that its centre of gravity is localized about  $0, 0, 1/4$ . The molecules 2 and 3 are joined with their pseudo-inversion related partners by the weak O–H...O bonds with the O...O distance of  $2.878(2) \text{ \AA}$ , forming planar dimers. The molecules 1 and 7 are displaced approximately perpendicularly to these dimers and the molecule 4 is displaced perpendicularly both to the dimers and to molecules 1 and 7. The geometric arrangement of these molecules is such that two succeeding aryl C–H bonds [mainly C(7)–H(7) and C(8)–H(8)] are directed towards the  $\pi$ -system of the neighbouring molecule yielding the so-called ‘T-shape’ type packing.<sup>23</sup> There is no contact shorter than  $3.5 \text{ \AA}$ , between non-hydrogen atoms of the set of molecules (1–3, 4 and 7) presented in Fig. 5, besides those within dimers. Instead, there are the C–H...O interactions in the second set of the molecules (1–3, 5 and 6) with C...O distance equal to  $3.360(5)$  and  $3.217(8) \text{ \AA}$ , respectively for O(1)...C(55) and O(5)...C(62) ( $x, y - 1, z$ ). These interactions are shown in Fig. 6, where the model of disordering assumed is illustrated.

## References

- 1 A. Awwal and F. Hibbert, *J. Chem. Soc., Perkin Trans. 2*, 1977, 152.
- 2 Z. Pawelka and L. Sobczyk, *J. Chem. Soc., Faraday Trans. 1*, 1980, 76, 43.
- 3 G. Hedestrand, *Z. Phys. Chem. B2*, 1929, 428.
- 4 A. J. Kirby and J. M. Percy, *Tetrahedron*, 1988, 44, 6903.
- 5 L. A. Weissberger and E. S. Proskauer, *Techniques of Organic Chemistry, Organic Solvents*, Interscience, New York, 1955, vol. VII.

- 6 G. M. Sheldrick, *Acta Crystallogr., Sect. A*, 1990, **46**, 467.
- 7 G. M. Sheldrick, SHELXL 93, *Program for the Refinement of Crystal Structures*, University of Göttingen, Germany, 1993.
- 8 *International Tables for Crystallography, Vol. C*, ed. A. J. Wilson, Kluwer Academic Publishers, Dordrecht, 1992.
- 9 A. Sucharda-Sobczyk and L. Sobczyk, *Bull. Acad. Pol. Sci. Ser. Sci. Chim.*, 1978, **26**, 549.
- 10 M. Rospenk and L. Sobczyk, *Magn. Reson. Chem.*, 1989, **27**, 445.
- 11 M. Ilczyszyn, L. Le-Van and H. Ratajczak, *Protons and Ions Involved in Fast Dynamic Phenomena*, Elsevier, Amsterdam 1978, p. 257.
- 12 T. Bisanz, *Roczniki Chem.*, 1963, **37**, 133.
- 13 J. W. Smith, *J. Chem. Soc.*, 1961, 81.
- 14 L. Sobczyk, H. Engelhardt and K. Bunzl, *The Hydrogen Bond*, eds. P. Schuster, G. Zundel and C. Sandorfy, North-Holland Publishing Company, Amsterdam, 1976, p. 937.
- 15 T. Pedersen, N. W. Larsen and L. Nygaard, *J. Mol. Struct.*, 1969, **4**, 59.
- 16 T. Głowiak, Z. Malarski, L. Sobczyk and E. Grech, *J. Mol. Struct.*, 1987, **157**, 329.
- 17 Z. Malarski, T. Lis, E. Grech, J. Nowicka-Scheibe and K. Majewska, *J. Mol. Struct.*, 1990, **221**, 227.
- 18 J. A. Kanters, A. Schouten, J. Kroon and E. Grech, *Acta Crystallogr., Sect. C*, 1991, **47**, 807.
- 19 J. A. Kanters, A. Schouten, A. J. M. Duisenberg, T. Głowiak, Z. Malarski, L. Sobczyk and E. Grech, *Acta Crystallogr., Sect. C*, 1991, **47**, 2148.
- 20 J. A. Kanters, E. H. Ter Horst, J. Kroon and E. Grech, *Acta Crystallogr., Sect. C*, 1992, **48**, 328.
- 21 M. L. Raves, J. A. Kanters and E. Grech, *J. Mol. Struct.*, 1992, **271**, 109.
- 22 T. Głowiak, E. Grech, Z. Malarski and L. Sobczyk, *J. Mol. Struct.*, 1993, **295**, 105.
- 23 J. Pawliszyn, M. M. Szczeniński and S. Scheiner, *J. Phys. Chem.*, 1984, **88**, 1726.

Paper 5/04805B

Received 21st July 1995

Accepted 26th September 1995